released from the gelatin hydrogel together with degraded gelatin fragments in the body, as a result of hydrogel degradation [23]. This release technology seems to be ideal for wound dressing material. Non-biodegradable materials may be responsible for the delay of wound healing because they remain as foreign bodies after slow release is finished. Fourth, to prepare bFGF incorporated into a gelatin sheet, air drying is not necessary, which may prevent bFGF from denaturing. Therefore, it is easy for the gelatin sheet to incorporate bFGF, enabling bFGF to regulate its biological functions. The gelatin sheet can be easily made to any sizes and shapes so as to be applicable for wound healing.

Well-organized granulation appeared in the bFGF(+) group on day 14, with many fibroblast cells, collagen fibers and capillaries. Two main signals, a 'competence' signal and a 'progression' signal, are needed for fibroblasts to start the synthesis of DNA [41]. The former does not promote DNA synthesis but changes G_0 and G_1 cells into competent cells capable of synthesizing DNA, while the latter activates the DNA synthesis of competent cells. The various fibroblast growth factors recognized to date are classified into these two categories [42]. As bFGF is classified as a 'competent factor', bFGF released from a gelatin sheet seems to increase the 'competent' fibroblast cells and promote granulation through 'competent cell' activation, but details of the mechanism by which bFGF promotes granulation are unknown.

Immunohistochemistry of mouse CD34 was used to count capillaries in our study because the antibody reacts with mouse CD34, a protein present on endothelial and hematopoietic progenitor cells. The antibody recognizes a neuraminidase-sensitive epitope on the endothelium *in vivo*, particularly in small vessels, neoformed capillaries and developing vascular structures in embryonal structures. Other methods exist for the evaluation of skin neovascularization: hemoglobin assay [18, 23, 43], and hematoxylin and eosin stain [44]. Hemoglobin assay requires skin to surround the wound, and hematoxylin and eosin stain is not specific for endothelial cells. Thus, we used mouse CD34 to identify capillary endothelial cells and to count the number of capillaries. The increase in capillary number observed on day 14 in the bFGF(+) group suggests that the bFGF contained in the gelatin sheet promoted angiogenesis. Recombinant human bFGF has been used clinically in Japan since 2001. In the present study, a 2-mm-thick gelatin sheet prevented wound exposure until 14 days. However, the natural polymers are usually weak in mechanical strength in the wet state. For a change for the better, the gelatin sheet may become a gauze substitute, offering outstanding recovery power with the capability of a controlled drug delivery system by combining it with cytokines, such as bFGF [45].

CONCLUSIONS

The gelatin sheet is effective for the controlled release of bFGF. bFGF incorporated into the gelatin sheet can promote wound healing, with a good balance of epithelialization and wound contraction, and accelerate granulation and neovascularization

when used to cover wounds. Moreover, gelatin sheets have a high water content, are biocompatible, biodegradable and easy to use, without the loss of bFGF bioactivity. These results indicate that the gelatin sheet containing bFGF is helpful not only for preventing infection but also for obtaining esthetically good results. The addition of other bioactive proteins to the gelatin sheet might be helpful for further reduction of the wound healing period.

Acknowledgements

We thank Dr. Mitsunori Ikeda and Dr. Hajime Kodama, Department of Dermatology, Program of Bioregulation and Genetics, Kochi Medical School Kochi University, for support and encouragement.

REFERENCES

1. D. Gospodarowicz, *Nature* **249**, 123 (1974).
2. D. Gospodarowicz, G. Neufeld and L. Schweigerer, *Cell Differ.* **19**, 1 (1986).
3. D. B. Rifkin and D. Moscatelli, *J. Cell Biol.* **109**, 1 (1989).
4. N. Gospodarowicz, *Ann. N.Y. Acad. Sci.* **638**, 1 (1991).
5. P. Buntrock, K. D. Jentzsch and G. Hender, *Exp. Pathol.* **21**, 62 (1982).
6. G. S. McGee, J. M. Cavidson, A. Buckley, A. Sommer, S. C. Woodward, A. M. Aquino, R. Barbour and A. A. Demetrious, *J. Surg. Res.* **45**, 145 (1988).
7. K. Mizuno, K. Yamamura, K. Yano, N. Takimoto and T. Sakurai, *Drug Deliv. Syst.* **13**, 49 (1998).
8. M. S. Hora, R. K. Rana, J. H. Nunberg, T. R. Tice, R. M. Gilley and M. E. Hudson, *Bio/Technology* **8**, 755 (1990).
9. P. J. Camarata, R. Suryanarayanan, D. A. Turner, R. G. Parke and T. J. Ebner, *Neurosurgery* **30**, 313 (1992).
10. W. R. Gombotz, S. C. Pankey, L. S. Bouchard, J. Ranchalis and P. Puolakkainen, *J. Biomater. Sci. Polymer Edn* **5**, 46 (1993).
11. J. C. Gautier, J. L. Grainger, A. Barbier, P. Dupont, D. Dussossoy, G. Pastor and P. Couvreur, *J. Control. Rel.* **20**, 67 (1992).
12. J. Murray, L. Brown, R. Langer and M. Klagsburn, *In vitro* **19**, 743 (1993).
13. E. B. Christine and W. M. Saltzman, *J. Control. Rel.* **24**, 15 (1993).
14. E. Ghezzo, L. M. Bendetti, M. Rochira, F. Biviano and L. Callegaro, *Int. J. Pharm.* **87**, 21 (1992).
15. E. R. Edelman, E. Mathiowitz, R. Langer and M. Klagsburn, *Biomaterials* **12**, 619 (1991).
16. R. J. Mumper, A. S. Hoffman, P. A. Puolakkainen, L. S. Bouchard and W. R. Gombota, *J. Control. Rel.* **30**, 241 (1994).
17. P. T. Goulmbek, R. Azhari, E. M. Jaffee, H. I. Livitsky, A. Lazenby, K. Leong and D. Paradoll, *Cancer Res.* **53**, 5841 (1993).
18. Y. Tabata, S. Hijikata and Y. Ikada, *J. Control. Rel.* **31**, 189 (1994).
19. K. Yamada, Y. Tabata, K. Yamamoto, S. Miyamoto, I. Nagata, H. Kikuchi and Y. Ikada, *J. Neurosurg.* **86**, 871 (1997).
20. Y. Tabata and Y. Ikada, *Proc. 4th Jpn. Int. SAMPE Symp.* **4**, 25 (1995).
21. A. Vais, *The Macromolecular Chemistry of Gelatin.* Academic Press, New York, NY (1964).
22. M. Yamamoto, Y. Tabata and Y. Ikada, *Drug Deliv. Syst.* **14**, 506 (1999).
23. Y. Tabata and Y. Ikada, *Adv. Drug Deliv. Rev.* **31**, 287 (1998).
24. Y. Tabata, A. Nagano and Y. Ikada, *Tissue Eng.* **5**, 127 (1999).
25. R. A. F. Clark, *J. Am. Acad. Dermatol.* **13**, 701 (1985).

26. A. Yoshida, T. Araki, T. Omata, I. Yamaguchi, K. Matsuda, T. Kurimoto and E. Tagashira, *Folia Pharmacol. Jpn.* **98**, 369 (1991).
27. D. G. Greenhalgh, K. H. Sprugel, M. J. Murray and R. Ross, *Am. J. Pathol.* **136**, 1235 (1990).
28. A. Furukawa, T. Yuge, K. Nakamura, Y. Nagashima and T. Awaji, *Kiso-to-Rinsho* **30**, 1579 (1996).
29. I. Ono, *J. Dermatol. Sci.* **29**, 104 (2002).
30. A. Iwakura, Y. Tabata, K. Nishimura, T. Nakamura, Y. Shimizu, M. Fujita and M. Komeda, *Ann. Thorac. Surg.* **70**, 824 (2000).
31. A. Iwakura, Y. Tabata, N. Tamura, K. Doi, K. Nishimura, T. Nakamura, Y. Shimizu, M. Fujita and M. Komeda, *Circulation* **104**, 1325 (2001).
32. Y. Cheng-Feng, Y. Tsutomu, K. Hideya, M. Hideki, H. Yoshihito, T. Yasuhiko, I. Yoshito and O. Yuichiro, *Ophthalm. Res.* **32**, 19 (2000).
33. B. Andrew and L. Nicholas, *Biochem. Biophys. Res. Commun.* **142**, 428 (1987).
34. K. E. Forsten, M. Fannon and M. A. Nugent, *J. Theor. Biol.* **205**, 215 (2000).
35. T. Elena, A. Ali, A. Achim, R. S. Matthew, M. Kevin, K. Alex and W. Anton, *J. Biol. Chem.* **276**, 40247 (2001).
36. M. Okada-Ban, P. T. Jean and J. Jacqueline, *Int. J. Biochem. Cell Biol.* **32**, 263 (2000).
37. E. Tanaka, K. Ase, T. Okuda, M. Okumura and K. Nogimori, *Biol. Pharm. Bull.* **19**, 1141 (1996).
38. M. David, *J. Biol. Chem.* **267**, 25803 (1992).
39. G. M. Luccioli, D. S. Kahn and H. R. Robertson, *Ann. Surg.* **160**, 1030 (1964).
40. D. M. Simpson and R. Ross, *J. Clin. Invest.* **51**, 2009 (1972).
41. C. D. Scher, R. C. Shepard, H. N. Antoniades and C. D. Stiles, *Biochim. Biophys. Acta* **560**, 217 (1979).
42. A. E. Postlethwaite and A. H. Kang, in: *Inflammation. Basic Principles and Clinical Correlates*, J. I. Gallin, I. M. Goldstein and R. Snydermann (Eds), p. 577. Raven Press, New York, NY (1988).
43. M. Okumura, T. Okuda, T. Nakamura and M. Yajima, *Biol. Pharm. Bull.* **19**, 530 (1996).
44. T. Ryoji and B. R. Daniel, *J. Exp. Med.* **172**, 245 (1990).
45. I. Kurokawa, J. Hayami and Y. Kita, *J. Int. Med. Res.* **31**, 149 (2003).

Journal of Molecular Diagnostics, Vol. 7, No. 1, February 2005

Epidermolysis Bullosa Simplex Associated with Pyloric Atresia Is a Novel Clinical Subtype Caused by Mutations in the Plectin Gene (*PLEC1*)

Hiroyuki Nakamura,* Daisuke Sawamura,* Maki Goto,* Hideki Nakamura,* James R. McMillan,* Susam Park,† Sumio Kono,‡ Shiro Hasegawa,‡ Son'e Paku,§ Tomohiko Nakamura,§ Yoshihumi Ogiso,¶ and Hiroshi Shimizu*

From the Department of Dermatology, Hokkaido University Graduate School of Medicine, Sapporo, Japan; the Division of Plastic Surgery† and the Division of Pediatric Surgery,‡ Shizuoka Children's Hospital, Shizuoka, Japan; and the Division of Neonatology§ and the Division of Clinical Pathology,¶ Nagano Children's Hospital, Toyoshina, Japan*

Epidermolysis bullosa (EB) is an inherited mechanobullous disorder of the skin, and is divided into three major categories: EB simplex (EBS), dystrophic EB, and junctional EB (JEB). Mutations in the plectin gene (*PLEC1*) cause EBS associated with muscular dystrophy, whereas JEB associated with pyloric atresia (PA) results from mutations in the α6 and β4 integrin genes. In this study, we examined three EB patients associated with PA from two distinct families. Electron microscopy detected blister formation within the basal keratinocytes leading to the diagnosis of EBS. Surprisingly, immunohistochemical studies using monoclonal antibodies to a range of basement membrane proteins showed that the expression of plectin was absent or markedly attenuated. Sequence analysis demonstrated four novel *PLEC1* mutations. One proband was a compound heterozygote for a nonsense mutation of Q305X and a splice-site mutation of 1344G→A. An exon-trapping experiment suggested that the splice-site mutation induced aberrant splicing of the gene. The second proband harbored a heterozygous maternal nonsense mutation, Q2538X and homozygous nonsense mutations R1189X. Analysis of the intragenic polymorphisms of *PLEC1* suggested that R1189X mutations were due to paternal segmental uniparental isodisomy. These results indicate that *PLEC1* is a possible causative gene in this clinical subtype, EBS associated with PA. Furthermore, two patients out of our three cases died in infancy. In terms of clinical prognosis, this novel subtype is the lethal variant in the EBS category. (*J Mol Diagn *2005, 7:28–35)*

Epidermolysis bullosa (EB) comprises a group of genetically determined skin fragility disorders characterized by blistering of the skin and mucous membrane. EB has traditionally been divided into three main categories on the basis of the level of tissue separation within the cutaneous basement membrane zone (BMZ); tissue separations in EB simplex (EBS), dystrophic EB and junctional EB (JEB) occur in the basal keratinocytes, the dermis, and the lamina lucida of basement membrane, respectively (Table 1).[1] Recent advances in EB research, have allowed the identification of mutations in 10 different genes, which account for the clinical heterogeneity in EB (Table 1).[2] Dominantly inherited EBS results from mutations in the basal keratinocyte-specific keratin 5 and 14 genes, whereas mutations in the plectin gene (*PLEC1*) can cause recessive EBS complicated by muscular dystrophy (EBS-MD). Dystrophic EB is characterized by severe blistering and scarring, and is due to mutations in the type VII collagen gene. The defective genes in JEB include the three genes encoding for the laminin 5 chains, the type XVII collagen gene, or the genes encoding the hemidesmosome-associated integrin α6 and β4 subunits (*ITGA6* and *ITGB4*).

The subtype of JEB involving α6 and β4 integrins is associated with congenital pyloric atresia (PA).[3,4,5] Staining with specific antibodies to the α6 or β4 integrin subunits in the JEB-PA skin reveals reduced or absent staining.[6,7] JEB-PA is usually lethal, but non-lethal variants have also been reported. The affected individuals with the lethal forms usually die within the first weeks or months after birth, whereas in the non-lethal variants, the clinical severity tends to improve with age.[3,5,8,9,10]

However, there have been several recent reports demonstrating EB cases associated with PA showing an intraepidermal level of cleavage consistent with the diagnosis of EBS.[11,12,13,14] In this study, we have encountered three

Supported by a Grant-In-Aid for Scientific Research (A) from the Japanese Society for the Promotion of Science (project no. 13357008 to H.S.), by a Health and Labor Sciences Research Grant (Research on Specific Diseases to H.S.) from the Ministry of Health Labor and Welfare of Japan, by a grant from the Japanese Society for the Promotion of Science (JSPS grant no. 00345 to J.R.M.), and by a grant-in-aid for JSPS fellows' research expenses (no. 00345).

Accepted for publication July 15, 2004.

Address reprint requests to Hiroshi Shimizu, Department of Dermatology, Hokkaido University Graduate School of Medicine, North 15, West 7, Sapporo 060-8638, Japan. E-mail: shimizu@med.hokudai.ac.jp.

Table 1. Epidermolysis Bullosa (EB) Classification and the Causative Genes[1]

Major EB type	Major EB subtypes	Involved genes/protein
EB simplex (EBS)	Dowling-Meara EBS	K5, K14
	Koebner EBS	K5, K14
	Weber-Cockayne EBS	K5, K14
	EBS with muscular dystrophy	Plectin
Junctional EB (JEB)	Herlitz JEB	Laminin 5
	Non-Herlitz JEB	Laminin 5, BPAG2
	JEB with pyloric atresia	$\alpha6\beta4$ integrin
Dystrophic EB (DEB)	Dominant DEB	Type VII collagen
	Hallopeau-Siemens recessive DEB	Type VII collagen
	Non-Hallopeau-Siemens recessive DEB	Type VII collagen

similar cases of EBS associated with PA that demonstrated an abnormal epidermal expression of plectin. Furthermore, we have identified novel four mutations, Q305X, 1344G→A, R1189X, Q2538X in the *PLEC1* gene of those cases. Thus, this study furthers our understanding of the possible range of pathophysiology in EB and of the biology of the cutaneous basement membrane.

Materials and Methods

Electron Microscopy

For electron microscopic examination, skin specimens were fixed in 5% glutaraldehyde and post-fixed in 1% osmium tetroxide, stained en-block in uranyl acetate. They were dehydrated in a graded series of ethanol solutions, then embedded in Araldite 6005 (NEM, Tokyo, Japan). Ultra-thin sections were cut, stained with uranyl acetate and lead citrate. The sections were examined with a transmission electron microscope (H-7100, Hitachi; Tokyo, Japan) at 75kv.

Immunofluorescence Studies

Direct immunofluorescence analysis using a series of antibodies against BMZ antigens and cryostat skin sections was performed as described previously.[6,15,16] The following monoclonal antibodies (mAbs) against BMZ components were used: mAbs HD1–121, K15, 10F6 and 5B3 against the rod domain of plectin; mAbs GoH3 and 3E1 (Chemicon International, CA) against the $\alpha6$ and $\beta4$ integrins, respectively; mAb GB3 (Sera-lab, Cambridge, UK) against laminin 5 antibody; mAb LH7.2 (Sigma, St. Louis, MO) against type VII collagen; mAb S1193 and HDD20 against BPAG1 and BPA2, respectively. The antibodies GoH3, S1193, and HDD 20 were kind gifts from Dr. A. Sonnenberg, the Netherlands Cancer Institute. The antibodies HD1–121 and K15 were kind gifts from Dr. K. Owaribe, Nogoya University.

Mutation Detection

Genomic DNA was obtained from both patients and the parents. The mutation detection strategy was performed after polymerase chain reaction (PCR) amplification of all exons and intron-exon borders, followed by direct automated nucleotide sequencing (Applied Biosystems, Foster City, CA). The genomic DNA nucleotides, the cDNA nucleotides and the amino acids of the protein were numbered based on the previous sequence information (GenBank Accession No. AH003623).[17] In particular, PCR amplification of exon 9, 12, 27, and one part of exon 32 was performed using following primers. Primers 5′-GTCGCTGTATGACGCCATGC-3′and 5′-TGGCTGGTAGCTCCATCTCC-3′ for exon 9 produced a 387-bp fragment of the genomic DNA extending from g.2717 to g.3103, primers 5′-CCCACTCGCCTTAGGACAGT-3′ and 5′-AAACCAACTCTGCCCAAAGC-3′ for exon 12 synthesized a 428-bp fragment from g.3571 to g.3998, primers 5′-TTTCGAGGCTGGGGCTTCAT-3′ and 5′-GCCTGGGTGATGGTGTGGTC-3′ for exon 27 synthesized a 771-pb fragment from g.9681 to g.10451, and primers 5′-TCTGCTTTGGTGGGTGATGG-3′and 5′-AGCCTCTGGTTCTCCTCAGC-3′ for a single part of exon 32 synthesized a 422-bp fragment from g.15326-g.15747. The PCR conditions of the amplification were 5 minutes at 94°C for one cycle, followed by 38 cycles of 45 seconds at 94°C, 30 seconds at 57°C or 60°C, and 1 minute at 72°C. The informed consents both for studies and publication of the photographs were obtained from both families in this study.

Verification of Mutations

Each mutation was confirmed by restriction enzyme digestion of PCR products. The Q305X and 1395G->A mutations resulted in the loss of a restriction site for the *Pst*I and *Hph*I, respectively. The R1189X mutation caused the generation of a new restriction enzyme site for *Tsp45*I.

There was no proper restriction enzyme to verify the Q2538X mutation. PCR amplification was carried out using the following PCR primers, 5-TCTGCTTTGGTGGGTGATGG-3 and 5-CTCCAGCTTGGCCTTCTCCA-3 for generation of a 225-bp product. We changed the last base of the latter primer (underlined) from the original sequence, so that the combination of this change and the upstream sequence created a new *Alu*I site in the PCR product. Since the Q2538X mutation was also located just one base upstream from that primer, Q2538X abolished this *Alu*I site.

Exon-Trapping Experiments

Exon trapping system (Invitrogen, Carlsbad, CA) is an approach used for the direct isolation of transcribed sequences from genomic DNA.[18] To generate a *PLEC1* genomic fragment extending from intron 10 to intron 13, we synthesized two primers, 5′-AAACTCGAGGGCTGTCCCAGGTCTGGT-3′ and 5′-ATTGGATCCTGGGGCCGTGTGTACCTG-3′ which contained the following restriction enzyme sites, *Xho*I and *Bam*HI, respectively. PCR was performed using genomic DNA from the proband 1 as a template. The DNA fragment was digested with *Xho*I and *Bam*HI and subcloned into the multi-cloning site of a pSPL3 expression vector, which contained a portion of the HIV-1 *tat* gene, an intron, splice donor and acceptor sites, and some flanking exon sequences. Sequence analysis selected constructs with or without the splice site mutation 1344G→A. The constructs were transfected into normal human epidermal keratinocytes using N-[1-(2,3-dioleoyloxy)propyl]-N,N,N-trimethylammonium methylsulfate (Roche Molecular Biochemicals). Total RNA was extracted from the culture cells and RT-PCR was performed using the trapping vector-specific oligonucleotide primers. The samples without transfection of the pSPL3 were used as controls. The PCR products were subcloned into a TA cloning vector pCR II (Invitrogen) and sequenced.

Results

Clinical Features of EB Associated with PA

The proband 1 was a male, born by spontaneous vaginal delivery after a 39-week gestation. His parents were unrelated and clinically normal. Pyloric atresia (PA) and polyhydramnios were suspected antenatally after ultrasound examination. Immediately after delivery, he presented with blisters and widespread ulcers on his trunk, genitalia, and legs. Findings from a routine abdominal radiograph led to a clinical diagnosis of EB associated with PA (Figure 1, A to C). Laparotomy revealed a severely distended stomach with a membrane at the pylorus. The membrane was excised and a pyloroplasty was performed. The histopathology of the septum showed re-epithelization of the epithelium, an atrophic lamina muscularis mucosae, and edematous submucosal tissue. He survived the operation, but still required intensive care at the age of 16 months. His elder brother, born 2 years before the proband 1, was also diagnosed as suffering from PA by routine abdominal X-ray. He manifested with multiple blisters and ulcers on his scalp, genitalia, and extremities, identical to those seen in the proband 1 (Figure 1, D to E). On the second day after birth, pyloroplasty and skin grafting were performed, but he later died of sepsis 4 months after birth.

The proband 2 was a female, born by induced vaginal delivery after a 36-week gestation, as the second child of non-consanguineous, healthy parents. She had a 1-year-old brother who was clinically unaffected. Antenatal ultrasonography had suggested a diagnosis of PA and

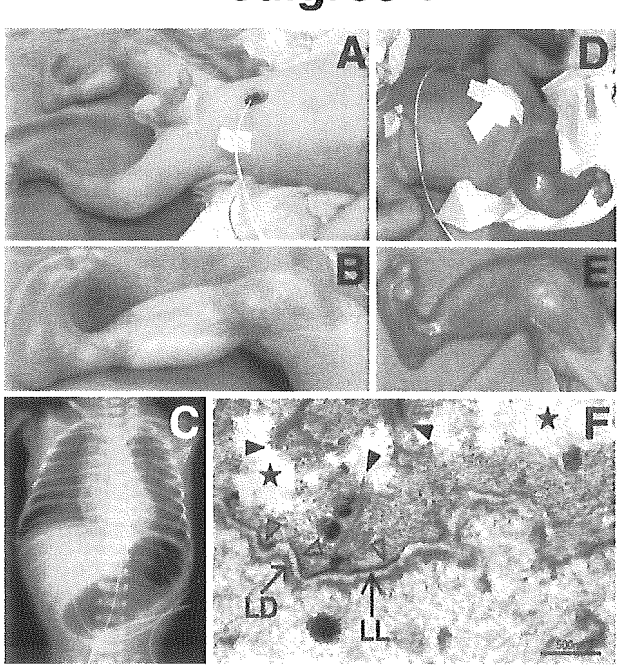

Figure 1. Clinical, X-ray, and ultrastructural findings of proband 1 in pedigree 1. **A:** Sharply demarcated erosions and ulcers on the trunk, genitalia, and lower extremity. **B:** Marked ulcers on the lower extremities. **C:** A single abdominal bubble of gas in an abdominal X-ray of proband 1. **D** and **E:** The same clinical manifestation of his elder brother. **F:** Electron microscopy of the skin from proband 1 shows tissue separation occurring at the base of the basal keratinocytes (**stars**). Keratin filaments are sparse and thin and not well associated with the hemidesmosome (HD) inner plaque (**full arrowheads**). Reduced numbers of hypoplastic HDs are recognized (**triangles**) and occasional HDs can be observed associated with thin bundles of keratin filaments within the basal keratinocyte (**open arrow**). The lamina densa (LD) and lamina lucida (LL) are present in the papillary dermis. **Bar**, 500 nm.

polyhydramnios. At birth, she presented with blisters and ulcers on the scalp, trunk, and extremities (Figure 2, A to D). Routine abdominal X-rays demonstrated a single abdominal bubble of gas, resulting in a clinical diagnosis of EB associated with PA. A laparotomy on the second day after birth showed a hugely distended stomach with a membrane at the pylorus. A gastroduodenostomy was subsequently performed. Histopathological analysis of the septum showed atrophic changes in general, normal appearance of the desquamative epithelium, and no increase in collagen fibers numbers. Due to her poor respiratory condition, she died of dyspnea at 31 days of age.

Skin Separation in Basal Keratinocytes

First, we examined the skin separation level within the epidermal BMZ. Electron microscopy of the skin samples from proband 1 revealed that the tissue separation was localized at the base of the basal keratinocytes and that hemidesmosomes (HDs) were reduced in frequency and hypoplastic (Figure 1F). In the skin sample from the proband 2 there was a reduction in HD numbers and many of the HDs appeared to be small or hypoplastic. The plane of separation was consistently within the basal keratinocyte, just above the HD inner plaque.[19] The ma-

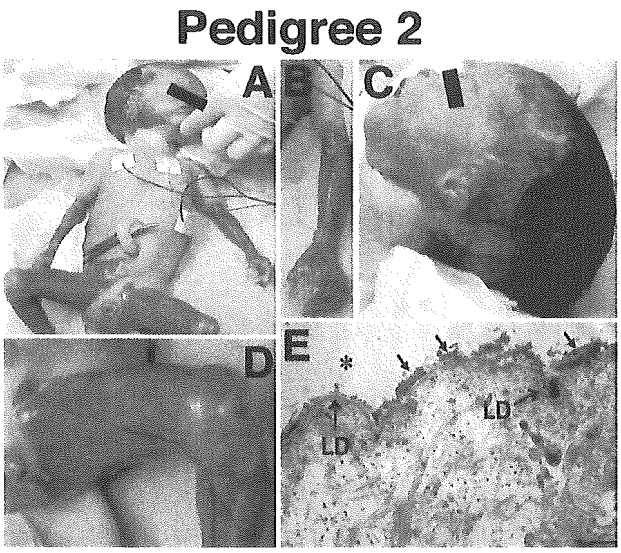

Figure 2. Clinical and ultrastructural findings of proband 2 in pedigree 2. **A:** Clearly demarcated blisters and ulcers on the scalp, abdomen, and extremities. **B:** Ulcers on the left arm. **C:** Localized erosions on the scalp. **D:** Ulcers on the left leg. **E:** Electron microscopy of the skin shows basal cell debris including flat electron densities (representing remnant hemidesmosome outer plaques (**arrows**) can be seen at the base of the intraepidermal split (**asterisk**). **Bar**, 1 μm.

jority of HD outer plaques remained attached to the underlying plasma membrane and extracellular electron-dense lamina densa. Keratin filaments within the basal cells appeared to form poor attachment to these rudimentary HDs, which remained firmly attached to the base of the separation (Figure 2E). The ultrastructural findings in both cases were consistent with these patients being classified as suffering from EBS.

Abnormal Expression of Plectin

An immunohistochemical study using monoclonal antibodies (mAbs) to a range of BMZ component proteins was performed (Figure 3). Immunoreactivity using the mAb HD1–121 against plectin was markedly attenuated in the proband 1 and completely lost in the proband 2. Analysis using other plectin mAbs K15, 10F6, and 5B5 revealed similar results, in which proband 1 showed markedly reduced expression while no immunoreactivity was detected in proband 2. Immunostaining for other BMZ proteins including the α6 and β4 integrins, laminin 5, type VII and IV collagens were normal (Figure 3). BPAG1 and BPAG2 also showed normal, bright, linear labeling of the BMZ in both probands (data not shown).

PLEC1 Mutations in Proband 1

Since abnormal expression of plectin was observed in both probands, we performed direct mutational analysis of the entire plectin gene. In this study, the cDNA nucleotides and the amino acids of the protein were numbered based on the previous sequence information (GenBank Accession No. AH003623).[17] Direct nucleotide sequencing of *PLEC1* from proband 1 demonstrated nonsense and splice-site mutations. The nonsense mutation was a C→T transition at nucleotide c.913 of cDNA in exon 9, resulting in the substitution of a glutamine (CAG) at position 305 with a stop codon (*T*AG) (Q305X). The splice-site mutation was a G→A substitution at nucleotide c.1344 in the cDNA that was located at the 3′ end of exon 12 (1344G→A) (Figure 4). The Q305X mutation was maternal and the 1344G→A mutation was paternal. These mutations were confirmed by restriction endonuclease analysis (Figure 4).

Since the splice site mutation of 1344G→A might just be a polymorphism, we examined 120 unrelated alleles as control and were unable to detected the same nucleotide change. Furthermore, we performed an exon-trapping experiment, as keratinocytes from the proband 1 or the parents were unavaliable. We inserted the genomic fragments with or without 1344G→A mutation into this vector, transfected these constructs into normal cultured human epidermal keratinocytes and prepared total RNA from the keratinocytes. We then synthesized cDNA, and amplified the extracted exons by PCR. Agarose gel electrophoresis showed strong 460-bp upper and weak lower 305-bp bands from the samples of the constructs containing the mutation, although a single 554-bp band was amplified from that construct without the mutation (data not shown).

Sequence analysis revealed that the upper 460-bp band contained exons 11 and 13 while the lower 305-bp band contained exon 11 alone. Conversely, exons 11, 12, and 13 were normally extracted from the DNA fragment without the mutation, resulting in a 554-pb band. Deletion of exon 12, which was 94 bp in size, caused a change in the mRNA coding frame and generation of a premature downstream stop codon. However, the combined size of exons 12 and 13 was 249 bp, so the deletion of these exons did not alter the coding frame and restored the translation of a polypeptide that was encoded by the downstream exons.

PLEC1 Mutations in Proband 2

Sequence analysis of the proband 2 revealed an unusual finding of both homozygous and heterozygous mutations. The homozygous mutation was a C→T transition at cDNA position c.3565 in exon 27, resulting in a substitution of an arginine (CGA) at residue 1189 with a stop codon (TGA) (R1189X). Conversely, the heterozygous mutation was a C→T transition at position c.7612 in exon 32, leading to an alteration of a glutamine (CAG) at 2538 to a stop codon (TAG) (Q2538X) (Figure 5). Nucleotide sequences of her parents disclosed that the father and mother were heterozygous for R1189X and Q2538X, respectively. These mutations were confirmed by restriction endonuclease analysis (Figure 5).

To eliminate a possibility that a sequence variation under one of the primers caused failure to amplify a maternal allele, we investigated by using a second set of primers for exon 27/intron 28. This also confirmed that the R1189X mutation was homozygous (data not shown).

Furthermore, comparison of 8 intragenic polymorphisms showed that the father and mother were heterozy-

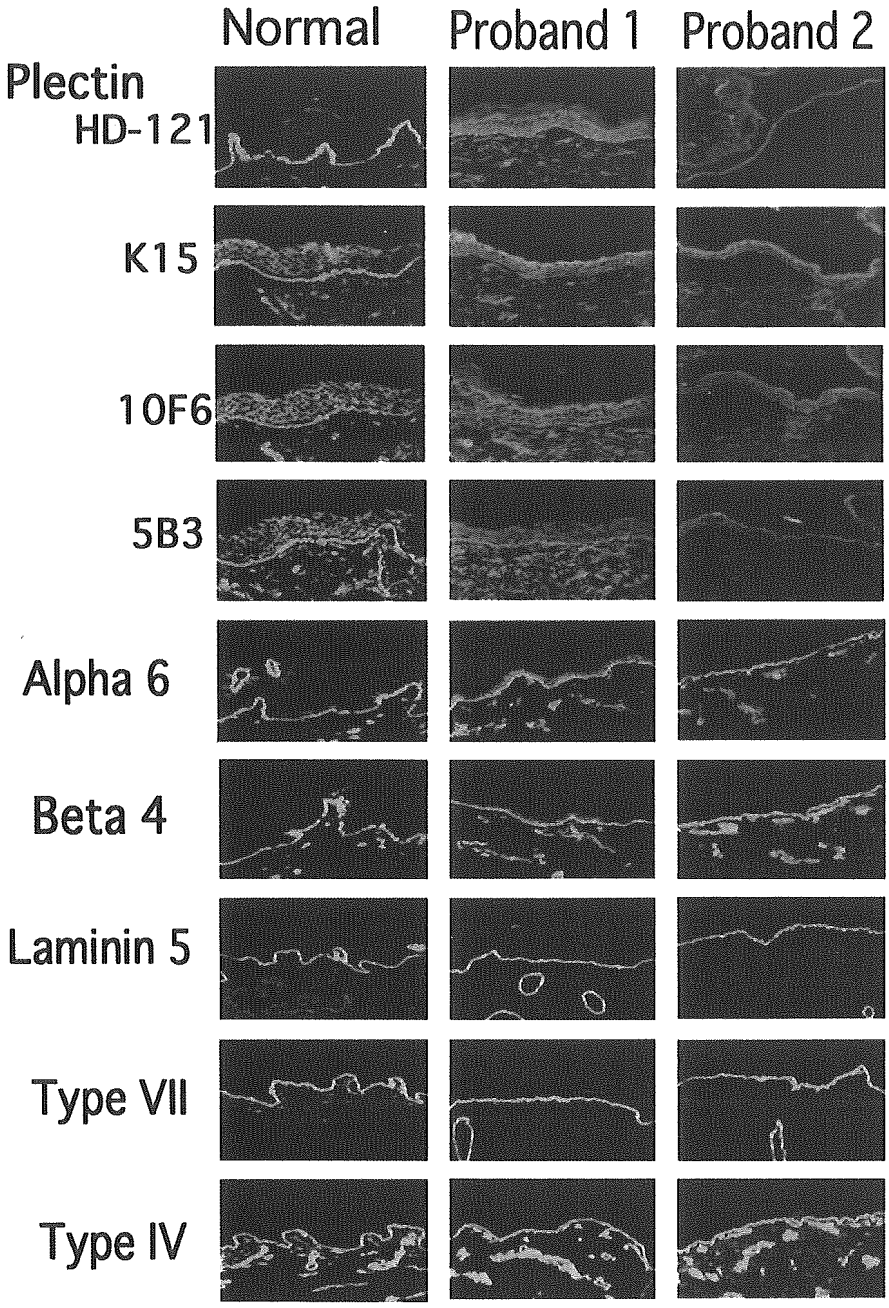

Figure 3. Immunofluorescence using antibodies against basement membrane zone components. Staining using HD1–121, K15, 10F6, and 5B3 monoclonal antibodies (mAbs) for plectin were markedly attenuated in the proband 1 and completely loss in the proband 2. Immunostaining for other proteins including $\alpha 6$ and $\beta 4$ integrins, laminin 5, type VII and IV collagens were normal in both probands and controls.

gous for 2 of 8 and 6 of 8 markers, respectively (Figure 6). The mutation R1189X and intron 28/10648 T→A were informative for the absence of a maternal allele in the proband 2. These results indicated that the mutations R1189X and their adjacent sequences were of paternal origin, suggesting possibility of segmental paternal uniparental isodisomy over this short area.

Discussion

Plectin, a component of the hemidesmosome (HD) inner plaque, is involved in the attachment and cross-linking of the cytoskeleton and intermediate filaments to specific membrane complexes.[20,21] Each monomer comprises a central rod domain of an α-helical coiled-coil structure and flanking amino-and carboxyl-terminal large globular domains.[22,23] It is widely distributed in almost all tissues and the exact function in each tissue is still unclear.[24,25] Although a family with EBS Ogna was reported to result from plectin mutation,[26] mutations in the plectin gene (*PLEC1*) generally cause EBS associated with muscular dystrophy (EBS-MD), which is characterized by generalized blistering, and a late-onset muscular dystrophy.[15,16,17,27,28,29]

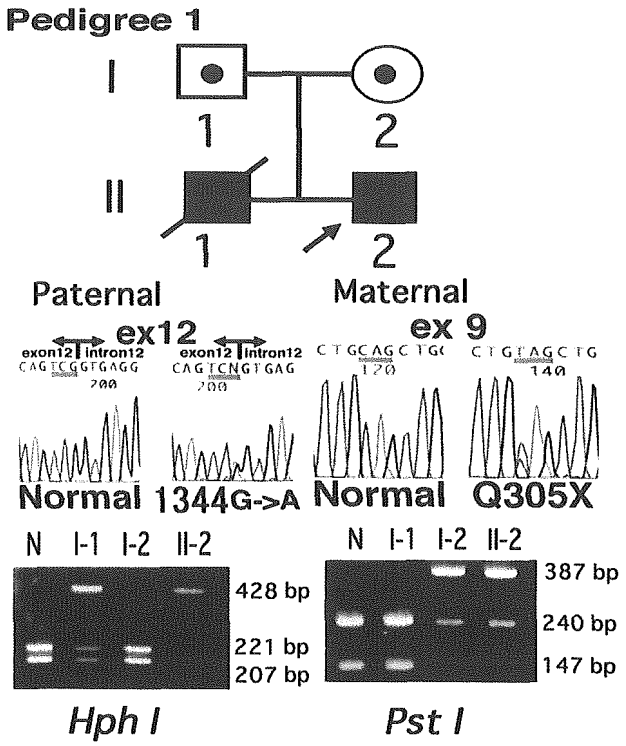

Figure 4. Mutation detection in pedigree 1. The proband harbored a G→A transition at position c.1344 in exon 12 within an intron-exon border (**middle-right panel**). He also possessed a heterozygous transition 913C→T (exon 9), leading to the substitution of glutamine 305 with a nonsense codon (Q305X). *HphI* digestion of the 428-bp fragment with and without the 1344G->A mutation product resulted in single band of 428 bp and double bands of 221 and 207 bp, respectively (**left panel**). The 387-bp PCR fragment containing the Q305X mutation was not digested by *PstI* whereas the digestion of the fragment without the mutation showed two bands of 240 and 147 bp (**right panel**). The 1344G→A mutation was paternal and the Q305X mutation was maternal.

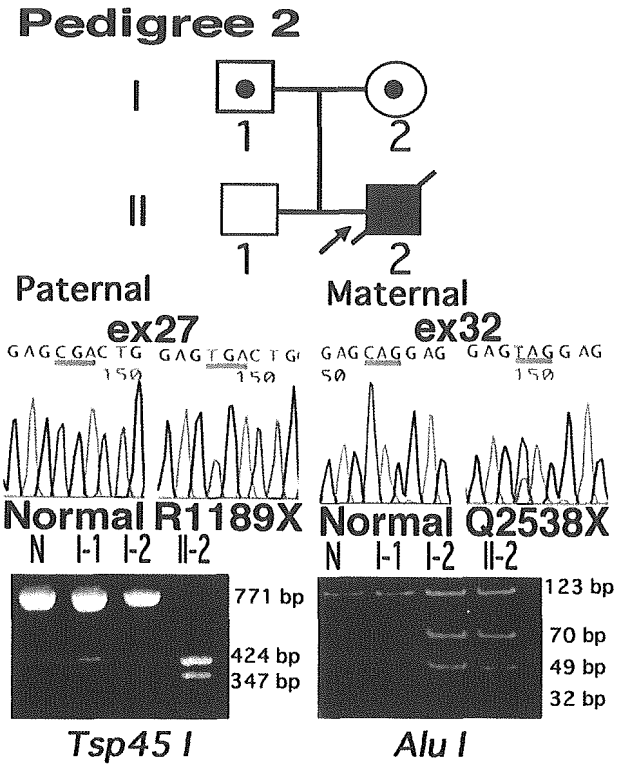

Figure 5. Mutation detection in pedigree 2. The proband 2 harbored a homozygous transition 3565C→T (exon 27) at codon 1189 producing a nonsense codon instead of arginine (R1189X) (**middle panel**). She also harbored a heterozygous C→T (c.7612) substitution (exon 32) in codon 2538, replacing glutamine with a nonsense codon (Q2538X). The R1189X mutation caused the generation of site for the *Tsp45I* restriction enzyme. The 771-bp PCR product with the mutation was digested by *Tsp45I* resulting in 424-bp and 347-bp bands (**left panel**). Since no proper restriction enzyme site was found around the Q2538X mutation, we changed one base of the PCR primer from the original sequence to create a site for *AluI* (see Materials and Methods). The digestion of 225-bp PCR product with Q2538X produced 70-bp band (**right panel**). The father and the mother are heterozygous for R1189X and Q2538X mutations, respectively.

The two probands in this study were both microscopically classified and clinically diagnosed as suffering from EBS associated with PA. We speculated at first, whether the causative mutations might lie in either *ITGA6* or *ITGB4* genes, known to cause PA-JEB. Surprisingly, however, the tissue separation was not within the lamina lucida as might be expected for JEB-PA, but was higher within basal keratinocyte, consistent with EBS. Immunohistochemical examination subsequently revealed abnormal plectin expression, leading us to speculate that mutations in *PLEC1* might be the underlying cause of this condition.

Indeed, mutational analysis detected novel nonsense and splice-site mutations on each *PLEC1* allele of the first proband (Figure 4). The splice-site mutation is thought to affect the splicing of the *PLEC1* gene, since the G nucleotide in the GT splice donor site in many human genes is relatively conserved within 78% of all splice junctions.[30] We first examined 120 unrelated alleles and could not detect the same nucleotide change. Furthermore, the exon-trapping experiments revealed that this mutation caused aberrant splicing of this region and suggested that this splice site mutation was likely to be pathogenic.

Immunofluorescence staining using the plectin antibodies, HD1–121, K15, 10F6, and 5B3, detected some plectin expression in proband 1 (Figure 3). HD1–121 recognizes multiple epitopes on the plectin rod domain.[31] In addition, the 10F6 and 5B3 epitopes were located in the central and carboxyl-terminal parts of the rod, respectively.[32] The 1344G→A mutation lies upstream of the region encoding the rod domain. As shown in the exon-trapping experiment, the presence of the low weaker band suggested some expression of the plectin

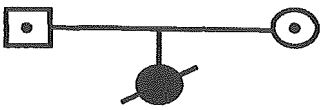

Exon 5/ 749 T→C	+	+	+	−	+	−
Intron 9/ 3023 C→G	+	+	+	−	+	−
Exon 15/ 4766 C→T	+	−	+	−	+	+
Intron 19/ 7407 T→C	+	+	+	−	+	−
Exon 27/ 10113(R1189X)	+	−	+	+	−	−
Intron 28/ 10648 T→A	+	+	+	+	−	−
Exon 31/ 12020 C →T	+	−	+	−	+	+
Exon 31/ 12271 T →C	+	+	+	−	+	−
Exon 32/ 15497(Q2538X)	−	−	−	+	+	−
Exon 32/ 15547 A →C	+	+	+	−	+	−

Figure 6. Detection of uniparental isodisomy. Comparison of 8 intragenic polymorphisms around the homozygous R1189 mutation showed that the father and the mother were heterozygous for 2 of 8 and 6 of 8 markers. The mutation R1189X and intron 28/10648 T→A were informative for the absence of a maternal allele in the proband.

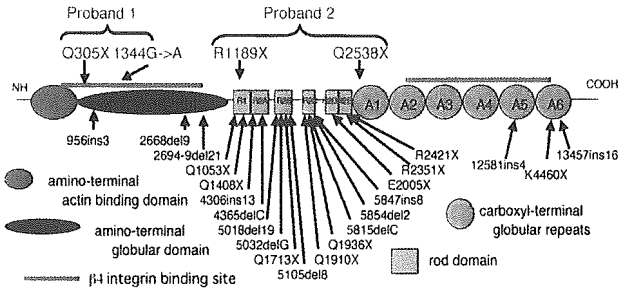

Figure 7. Database showing the position of mutations in *PLEC1*. Each functional domain is shown in the schematic model of plectin structure. The cDNA and the amino acids of the protein are numbered based on the previous sequence information (GenBank Accession No. AH003623).[17] Amino-terminal actin binding domain, amino-terminal globular domain, β4 integrin binding sites, rod domain, and carboxyl-terminal globular domain are shown.

rod domain, which is expected to be insufficient for the normal function of plectin.

Although we found nonsense mutations of both paternal and maternal origins in proband 2, it was unusual that R1189X mutation was homozygous. To further understand the mechanism causing this defect, we searched for several intragenic polymorphisms within the *PLEC1* gene (Figure 6). The results suggested that the R1189X mutations and their adjacent sequences had originated from one paternal allele. Uniparental disomy refers to the situation in which two copies of a chromosome come from the same parent.[33] The possibility of isodisomy can be hypothesized if two identical segments from one parental homologue are present in the offspring, whereas sequences of both homologues from the transmitting parent are present in the normal cause, heterodisomy. Angelman syndrome and Prader-Willi syndrome are examples of disorders caused by uniparental disomy.[34] This study indicates that the R1189X mutations and its adjacent sequences are likely to be derived from one paternal homologue and suggested possibility of segmental uniparental paternal isodisomy.

The next point we should discuss was how *PLEC1* mutation led to PA. We have reviewed the previously reported cases of plectin mutations in EBS-MD. In total, there were 22 mutations, of those, 16 mutations resided within the region encoding the rod domain (Figure 7). Of the 4 novel mutations from our cases, roughly, Q305X, 1344G->A, and Q2538X were not within the rod domain region and R1189X was in the very end of this domain. Plectin interacts with the cytoplasmic tail of β4 integrin via its carboxyl as well as amino-terminal domains (Figure 7),[23,35] and mutations in the β4 integrin gene result in PA. Therefore, we postulated that the development of PA in our cases is closely linked with the functions of plectin and the β4 integrin subunit. Interestingly, the mutations Q305X and 1344G→A in the first proband resided in the amino-terminal binding site for β4 integrin (Figure 7). However, the mutations of the second proband were not in the β4 integrin-binding site.

The level of tissue separation in EBS due to plectin gene mutations is different from that due to K5 or K14 gene mutations. In the latter cases there is a global cytolysis of the basal keratinocytes, while in case of the patients with *PLEC1* mutations the tissue separation is very low at the level of hemidesmosomes. Also, molecular consequences of deletion of the cytoplasmic domain of β4 integrin subunit or the type XVII collagen caused predominant features of EBS with intraepidermal separation.[36,37] Therefore, some investigators have proposed hemidesmosomal variants that include EBS with muscular dystrophy, JEB with pyloric atresia and generalized atrophic benign EB[2]. In this aspect, EBS with pyloric atresia in this study would belong to the variants.

Molecular mechanism of PA development even in JEB-PA has not yet been fully elucidated although phenotype and genotype information of this disease has been accumulated. Targeted ablation of both the *ITGA4* and *ITGB6* genes in mice clearly induced separation of the epidermis from the dermis as seen in the skin of JEB-PA.[38,39,40] In contrast, those model mice could not show straightforward evidence concerning mechanism of PA. Further studies are needed to clarify the pathogenesis of PA in all patients with EBS-PA as well as those with JEB-PA.

In this study, we have demonstrated for the first time that *PLEC1* mutations induce novel subtype of EB, EBS-PA. No definite conclusion has yet been reached regarding the occurrence of late onset muscular dystrophy phenotype of our three cases, since two patients have already died and one patient is still a neonate. However, this study furthers our understanding of the possible range of pathophysiology in EB and of the biology of the cutaneous basement membrane. In the previously reported four cases of EBS-PA,[11,12,13,14] two cases[11,12] also died shortly after birth although a search for plectin mutations were not carried out. In terms of clinical prognosis, this novel subtype EBS-PA is the lethal variant in the EBS category and will become a real target for gene therapy in the near future.

Acknowledgments

We thank the patients and their family for their interest in our study and the referring physicians for providing clinical information.

References

1. Fine JD, Eady RA, Bauer EA, Briggaman RA, Bruckner-Tuderman L, Christiano A, Heagerty A, Hintner H, Jonkman MF, McGrath J, McGuire J, Moshell A, Shimizu H, Tadini G, Uitto J: Revised classification system for inherited epidermolysis bullosa: report of the Second International Consensus Meeting on diagnosis and classification of epidermolysis bullosa. J Am Acad Dermatol 2000, 42:1051–66
2. Pulkkinen L, Uitto J: Mutations analysis and molecular genetics of epidermolysis bullosa. Matrix Biol 1999, 18:29–42
3. Vidal F, Aberdam D, Miquel C, Christiano AM, Pulkkinen L, Uitto J, Ortonne JP, Meneguzzi G: Integrin beta 4 mutations associated with junctional epidermolysis bullosa with pyloric atresia. Nat Genet 1995, 10:229–234
4. Ruzzi L, Gagnoux-Palacios L, Pinola M, Belli S, Meneguzzi G, D'Alessio M, Zambruno G: A homozygous mutation in the integrin alpha6 gene in junctional epidermolysis bullosa with pyloric atresia. J Clin Invest 1997, 99:2826–2831
5. Pulkkinen L, Kimonis VE, Xu Y, Spanou EN, McLean WH, Uitto J:

Homozygous alpha6 integrin mutation in junctional epidermolysis bullosa with congenital duodenal atresia. Hum Mol Genet 1997, 6:669–674
6. Shimizu H, Suzumori K, Hatta N, Nishikawa T: Absence of detectable alpha 6 integrin in pyloric atresia-junctional epidermolysis bullosa syndrome: application for prenatal diagnosis in a family at risk for recurrence. Arch Dermatol 1996, 132:919–925
7. Brown TA, Gil SG, Sybert VP, Lestringant GG, Tadini G, Caputo R, Carter WG: Defective integrin alpha 6 beta 4 expression in the skin of patients with junctional epidermolysis bullosa and pyloric atresia. J Invest Dermaol 1996, 132:919–925
8. Nissen CM, van der Raaij-Helmer MH, Hulsman EH, van der Neut R, Jonkman MF, Sonnenberg A: Deficiency of the integrin beta 4 subunit in junctional epidermolysis bullosa with pyloric atresia: consequences for hemidesmosome formation and adhesion properties. J Cell Sci 1996, 109:1695–1706
9. Mellerio JE, Pulkkinen L, McMillan JR, Lake BD, Horn HM, Tidman MJ, Harper JI, McGrath JA, Uitto J, Eady RA: Pyloric atresia-junctional epidermolysis bullosa syndrome: mutations in the integrin $\beta 4$ gene (ITGB4) in two unrelated patients with mild disease. Br J Dermatol 1998, 139:862–871
10. Ashton GH, Sorelli P, Mellerio JE, Keane FM, Eady RA, McGrath JA: Alpha6 beta4 integrin abnormalities in junctional epidermolysis bullosa with pyloric atresia. Br J Dermatol 2001, 144:408–414
11. Cowton JA, Beattie TJ, Gibson AA, Mackie R, Skerrow CJ, Cockburn F: Epidermolysis bullosa in association with aplasia cutis congenital and pyloric atresia. Acta Paediatr Scand 1982, 71:155–160
12. Gire C, Nicaise C, Minodier P, Meneguzzi G, Prost C, Souia F: Epidermolysis bullosa and pyloric atresia. Acta Paediatr 1999, 88: 105–106
13. Kim DK, Kim SC, Chang SN, Kim SY: Epidermolysis bullosa simplex (Dowling-Meara type) associated with pyloric atresia and congenital urologic abnormalities. Yonsei Med J 2000, 41:411–415
14. Morrell DS, Rubenstein DS, Briggaman RA, Fine JD, Pulkkinen L, Uitto J: Congenital pyloric atresia in a newborn with extensive aplasia cutis congenital and epidermolysis bullosa simplex. Br J Dermatol 2000, 143:1342–1343
15. Smith FJ, Eady RA, Leigh IM, McMillan JR, Rugg EL, Kelsell DP, Bryant SP, Spurr NK, Geddes JF, Kirtschig G, Milana G, de Bono AG, Owaribe K, Wiche G, Pulkkinen L, Uitto J, Mclean WH, Lane EB: Plectin deficiency results in muscular dystrophy with epidermolysis bullosa. Nat Genet 1996, 13:450–457
16. Shimizu H, Takizawa Y, Pulkkinen L, Murata S, Kawai M, Hachisuka H, Udono M, Uitto J, Nishikawa T: Epidermolysis bullosa simplex associated with muscular dystrophy: phenotype-genotype correlation and review of the literature. J Am Acad Deramtol 1999, 41:950–956
17. McLean WH, Pulkkinen L, Smith FJ, Rugg EL, Lane EB, Bullric F, Burgeson RE, Amano S, Hudson DL, Owaribe K, McGrath JA, McMillan JR, Eady RA, Leigh IM, Christiano AM, Uitto J: Loss of plectin causes epidermolysis bullosa with muscular dystrophy: cDNA cloning and genomic organization. Genes Dev 1996, 10:1724–1735
18. Buckler AJ, Chang DD, Graw SL, Brook JD, Haber DA, Sharp PA, Housman DE: Exon amplification: a strategy to isolate mammalian genes based on RNA splicing. Proc Natl Acad Sci USA 1991, 88: 4005–4009
19. McMillan JR, McGrath JA, Tidman MJ, Eady RA: Hemidesmosomes show abnormal association with the keratin filament network in junctional forms of epidermolysis bullosa. J Invest Dermatol 1998, 110: 132–137
20. Klatte DH, Kurpakus MA, Grelling KA, Jones JCR: Immunochemical characterization of three components of the hemidesmosome and their expression in cultured epithelial cells. J Cell Biol 1989, 109: 3377–3390
21. Borradori L, Sonnenberg A: Structure and function of hemidesmosome: more than simple adhesion complexes. J Invest Dermatol 1999, 112: 411–41
22. Liu CG, Maercker C, Castanon MJ, Hauptmann R, Wiche G: Human plectin: organization of the gene, sequence analysis, and chromosome localization (8q24). Proc Natl Acad Sci USA 1996, 93:4278–4283
23. Wiche G: Role of plectin in cytoskeleton organization and dynamics. J Cell Sci 1998, 111:2477–2486
24. Wiche G, Krepler R, Artlieb U, Pytela R, Denk H: Occurrence and immunolocalization of plectin in tissues. J Cell Biol 1983, 97:887–901
25. Uitto J, Pulkkinen L, Smith FJ, McLean WHI: Plectin and human genetic disorders of the skin and muscle: the paradigm of epidermolysis bullosa with muscular dystrophy. Exp Dermatol 1996, 5:237–246
26. Koss-Harnes D, Hoyheim B, Anton-Lamprecht I, Gjesti A, Jorgensen RS, JahnsenFL, Olaisen B, Wiche G, Gedde-Dahl Jr T: A site-specific plectin mutation causes dominant epidermolysis bullosa simplex Ogna: two identical de novo mutations. J Invest Dermatol 2002, 118:87–93
27. Chavanas S, Pulkkinen L, Gache Y, Smith FJ, Mclean WH, Uitto J, Ortonne JP, Meneguzzi G: A homozygous nonsense mutation in the PLEC1 gene in patients with epidermolysis bullosa simplex with muscular dystrophy. J Clin Invest 1996, 98:2196–2200
28. Gache Y, Chavanas S, Lacour JP, Wiche G, Owaribe K, Meneguzzi G, Ortonne JP: Defective expression of plectin/HD1 in epidermolysis bullosa simplex with muscular dystrophy. J Clin Invest 1996, 97: 2289–2298
29. Pulkkinen L, Smith FJD, Shimizu H, Murata S, Yaoita H, Hachisuga H, Nishikawa T, McLean WHI, Uitto J: Homozygous deletion mutations in the plectin gene (PLEC1) in patients with epidermolysis bullosa simplex associated with late-onset muscular dystrophy. Hum Mol Genet 1996, 5:1539–1546
30. Shapiro MB, Senapathy P: RNA splice junctions of different classes of eukaryotes: sequence statistics and functional implications in gene expression. Nucleic Acids Res 1987, 15:7155–7174
31. Okumura M, Uematsu J, Hirako Y, Nishizawa Y, Shimizu H, Kido N, Owaribe K: Identification of the hemidesmosomal 500 kDa protein (HD1) as plectin. J Biochem 1999, 126:1144–1150
32. Foisner R, Feldman B, Sander L, Seifert G, Artlieb U, Wiche G: A panel of monoclonal antibodies to rat plectin: distinction by epitope mapping and immunoreactivity with different tissues and cell lines. Acta Histochem 1994, 96:421–438
33. Kotzot D: Complex and segmental uniparental disomy (UPD): review and lessons from rare chromosomal complements. J Med Genet 2001, 38:497–507
34. Cassidy SB, Schwartz S: Prader-Willi and Angelman syndromes: disorders of genomic imprinting. Medicine 1998, 77:140–151
35. Schaapveld RQ, Borradori L, Geerts D, van Leusden MR, Kuikman I, Nievers MG, Niessen CM, Steenbergen RD, Snijders PJ, Sonnenberg A: Hemidesmosome formation is initiated by the beta4 integrin subunit, requires complex formation of beta4 and HD1/plectin, and involves a direct interaction between beta4 and the bullous pemphigoid antigen 180. J Cell Biol 1998, 142:271–284
36. Fontao L, Tasanen K, Huber M, Hohl D, Koster J, Bruckner-Tuderman L, Sonnenberg A, Borradori L: Molecular consequences of deletion of the cytoplasmic domain of bullous pemphigoid 180 in a patient with predominant features of epidermolysis bullosa simplex. J Invest Dermatol 2004, 122:65–72
37. Jonkman MF, Pas HH, Nijenhuis M, Kloosterhuis G, Steege G: Deletion of a cytoplasmic domain of integrin beta4 causes epidermolysis bullosa simplex. J Invest Dermatol 2002, 119:1275–1281
38. van der Neut R, Krimpenfort P, Calafat J, Niessen CM, Sonnenberg A: Epithelial detachment due to absence of hemidesmosomes in integrin beta 4 null mice. Nat Genet 1996, 13:366–369
39. Georges-Labouesse E, Messaddeq N, Yehia G, Cadalbert L, Dierich A, Le Meur M: Absence of integrin alpha 6 leads to epidermolysis bullosa and neonatal death in mice. Nat Genet 1996, 13:370–373
40. Murgia C, Blaikie P, Kim N, Dans M, Petrie HT, Giancotti FG: Cell cycle and adhesion defects in mice carrying a targeted deletion of the integrin 4 cytoplasmic domain. EMBO J 1998, 17:3940–3951

and dermatan sulfate,[14] suggesting that diabetes in these patients can influence the composition of connective tissue.

In our patient, it is clear that both conditions, scleredema and AN, are linked to an insulin-resistant state evidenced by his uncontrolled diabetes. The patient's family history, the duration of the lesion (years), coupled with difficulty managing his diabetes suggests that his scleredema and AN are related to insulin resistance. The lesion first appeared when the patient was 55 years old. It is well established that insulin resistance increases with age.[15] Also, the lesion did not resolve itself, as scleredema often does, but remained the same for many years. To date, our patient's lesions have not changed.

Acanthosis nigricans and scleredema have been reported in the same area in one previously published case associated with multiple myeloma.[1] In our patient, both the AN and scleredema coexist within the same area of skin. Acanthosis nigricans usually occurs in intertriginous areas. In this case, the indurated plaque of scleredema on the back creates a pseudointertriginous area that may have predisposed the formation of AN. Furthermore, both disorders have developed together over the same period of time and both have remained fairly static as neither condition has shown improvement even with more aggressive antidiabetic therapy. While their course may seem coincidental, we believe they are tied together by this patient's inability to sufficiently control his diabetes.

References

1 Valente L, Velho GC, Farinha F, *et al.* Scleredema, acanthosis nigricans, and IgA/Kappa multiple myeloma. *Ann Dermatol Venereol* 1997; 124: 537–539.

2 Schwartz RA. Acanthosis nigricans. *J Am Acad Dermatol* 1994; 31: 1.

3 Kahn CR, Flier JS, Bar RS, *et al.* The syndromes of insulin resistance and acanthosis nigricans: insulin receptor disorders in man. *N Engl J Med* 1983; 34: 145–150.

4 Hud JA Jr, Cohen JB, Wagner JM, *et al.* Prevalence and significance of acanthosis nigricans in an adult obese population. *Arch Dermatol* 1992; 128: 941–944.

5 Brown J, Winkelmann RK, Acanthosis nigricans. A study of 90 cases. *Medicine (Baltimore)* 1968; 47: 33.

6 Fleming MG, Simon SI. Cutaneous insulin reaction resembling acanthosis nigricans. *Arch Dermatol* 1986; 122: 1054.

7 Blundell TL, Bedarkian S, Humbel RE. Tertiary structure receptor binding, and antigenicity of insulin-like growth factor. *Fed Proc* 1983; 42: 2592–2597.

8 Flier JS. Metabolic importance of acanthosis nigricans. *Arch Dermatol* 1985; 121: 193–194.

9 Cruz PD Jr, Hud JA Jr. Excess insulin binding to insulin-like growth factor receptors: proposed mechanism for acanthosis nigricans. *J Invest Dermatol* 1992; 98: 82S–85S.

10 Kahn RC, Flier JS. The syndromes of insulin resistance and acanthosis nigricans. *N Engl J Med* 1976; 294: 739–745.

11 Graff R. Discussion of scleredema adultorum. *Arch Dermatol* 1968; 98: 319–320.

12 Cohn BA, Wheeler CE, Briggaman A. Scleredema adultorum of Bushke and diabetes mellitus. *Arch Dermatol* 1970; 101: 27–35.

13 Fleischmajer R, Faludi G, Krol S. Scleredema and diabetes mellitus. *Arch Dermatol* 1970; 101: 21–35.

14 Silbert C, Kleinman HK. Studies of cultured human fibroblasts in diabetes mellitus. Changes in heparan sulfate. *Diabetes* 1979; 28: 61–64.

15 DeFronzo RA. Glucose intolerance and aging. Evidence for tissue sensitivity to insulin. *J Clin Invest* 1979; 28: 1095–1101.

Cameo

Metastasis of lung cancer to the finger: a report of two cases

Hiroyuki Nakamura, MD, Tadamichi Shimizu, MD, Kazuo Kodama, MD, and Hiroshi Shimizu, MD

From the Department of Dermatology, Hokkaido University Graduate School of Medicine, Kita-ku, Japan

Correspondence
Tadamichi Shimizu, MD
Department of Dermatology
Hokkaido University Graduate School of Medicine
North 15, West 7
Kita-ku, 060-8638
Japan
E-mail: michiki@med.hokudai.ac.jp

Case 1 A 73-year-old man complained of a 2-month history of an asymptomatic nodule on the left thumb. The nodule had enlarged gradually and was accompanied by tenderness. The nodule on the tip of the left thumb was about 1 cm in diameter, well demarcated, fleshy, and reddish, with a granulomatous appearance (Fig. 1a). Histopathologic findings of the digital nodule revealed a dense dermal infiltration of cells with a marked nuclear atypicality, cell keratinization, and intercellular bridges (Fig. 1b). Because the diagnosis of a metastatic carcinoma of the skin was suspected, subsequent systemic examination was considered. Computed tomography revealed the presence of a primary carcinoma in the left lung, which was diagnosed as squamous cell carcinoma, T4N0M1, stage IV, and there were multiple metastases. The histopathologic finding of the digital nodule was similar to that of the lung lesions. The patient underwent radiation therapy for the digital tumor, and systemic

chemotherapy which was stopped because of adverse side-effects. The patient died 6 months after identification of the tumor.

Case 2 A 71-year-old man presented with a nodule on the left ring finger 1 month after operation for cancer of the left lung. Pathologic findings of the lung revealed a moderate or highly differentiated squamous cell carcinoma with cell keratinization, pT2N1M0, stage II. The finger tumor gradually enlarged in size. Physical examination showed an approximately 2 cm in diameter, elastic, hard, relatively well-demarcated, and hyperkeratotic tumor on the tip of the left ring finger (Fig. 2a). The lesion was accompanied by erosions in its center and a dark, erythematous swelling at the surrounding edges. A skin biopsy of the digital tumor was taken. Histologic examination revealed a dense dermal infiltration with marked nuclear atypicality and a tendency to keratinize. Squamous cell carcinoma with moderate or high cell differentiation was pathologically diagnosed (Fig. 2b), the same as recognized in the lung cancer specimen. This case was diagnosed as metastatic carcinoma to the finger, associated with primary lung cancer.

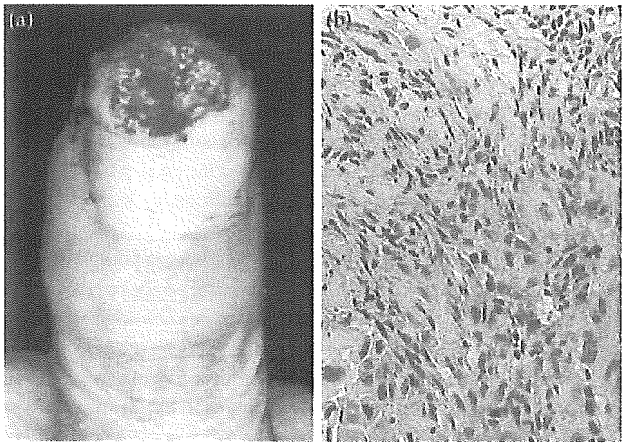

Figure 1 (a) Clinical appearance of Case 1. Tumor on the tip of the left thumb. (b) Histopathology of the tumor of Case 1 showing dense dermal infiltration of the cells, with marked nuclear atypicality, cell keratinization, and intercellular bridges (hematoxylin and eosin staining; original magnification, × 40)

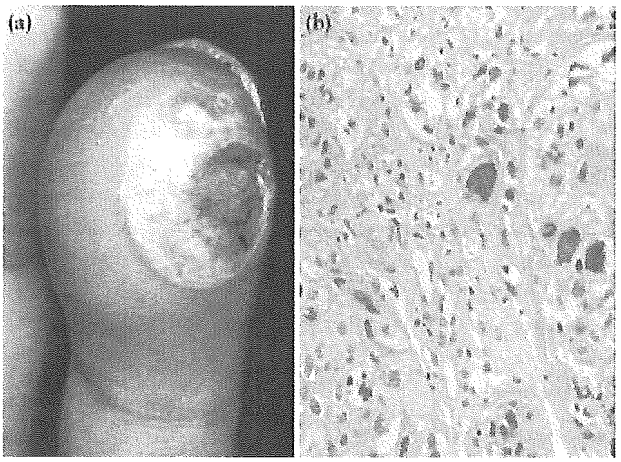

Figure 2 (a) Clinical appearance of Case 2. Tumor on the tip of the left ring finger with an erosion at its center and an erythematous swelling at the surrounding edges. (b) Skin biopsy from the nodule of Case 2 showing the proliferation of marked atypical squamous cells in the dermis and keratinization of the cells (hematoxylin and eosin staining; original magnification, × 40)

Discussion

Until now, 138 cases of metastasis to digital skin have been reported;[1,2] however, in only 17 cases have the digital metastases been recognized before the diagnosis of primary cancer, as in Case 1.[1] Fifty-six of the 138 cases (39.9%) showed lung cancer as the primary tumor.[1,2] We need to distinguish between digital metastases and primary squamous cell carcinomas. Squamous cell carcinomas metastatic to the skin are usually located within the dermis and/or the subcutaneous fat with no connection to the epidermis histopathologically.[1–3] In our cases, histologic examination revealed tumor nests extending to the upper dermis with the absence of proliferation from the epidermis. There have been many cases with invasion of carcinoma to the phalanx.[1,2,4] The average period from the recognition of primary cancer to the diagnosis of metastasis to the finger was 18 months (range, 2 weeks to 7 years).[1,4] The mean survival after the recognition of the digital metastasis was approximately 4 months.[2,4,5]

The therapy for cutaneous lesions is not well defined. Most patients with metastatic carcinoma to the finger are followed up without special treatment for the lesions,[2,4,6] but some have undergone radiation,[2] or even amputation of the digit with the metastatic tumor.[2,7,8] There have been cases of the metastasis of renal cell carcinoma in which amputation or wide excision has contributed to the potential for long-term survival.[4] In Case 1, the patient underwent radiation for the cutaneous lesion for the purpose of pain management.

It may be possible to increase the survival of patients with digital metastases with the use of appropriate treatment. Therefore, when a digital nodule is encountered, metastatic carcinoma to the skin should always be included in the

differential diagnosis, even if the individual has never been diagnosed as having cancer.

References

1 Baran R, Guillot P, Tosti A. Metastasis from carcinoma of the bronchus to the distal aspect of two digits. *Br J Dermatol* 1998; 138: 708.

2 Cohen PR. Metastatic tumors to the nail unit; subungual metastases. *Dermatol Surg* 2001; 27: 280–293.

3 Elder D, *et al. Lever's Histopathology of the Skin*, 8th edn. Philadelphia: Lippincott-Raven Publishers, 1997: 1011–1018.

4 Umebayashi Y. Metastasis of esophageal carcinoma manifesting as whitlow-like lesions. *J Dermatol* 1998; 25: 256–259.

5 Galmarini CM, Kertesz A, Oiva R, *et al.* Metastasis of bronchogenic carcinoma to the thumb. *Med Oncol* 1998; 15: 282–285.

6 Okada H, Qing J, Ohnishi T, *et al.* Metastasis of gastric carcinoma to a finger. *Br J Dermatol* 1999; 140: 776–777.

7 Ghert MA, Harrelson JM, Scully SP. Solitary renal cell carcinoma metastasis to the hand: the need for wide excision or amputation. *J Hand Surg* 2001; 26A: 156–160.

8 Shannon FJ, Antonescu CR, Athanasian EA. Metastatic thymic carcinoma in a digit: a case report. *J Hand Surg* 2000; 25: 1169–1172.

Ultrastructural Features of Trafficking Defects Are Pronounced in Melanocytic Nevus in Hermansky–Pudlak Syndrome Type 1

Ken Natsuga,* Masashi Akiyama,* Tadamichi Shimizu,* Tamio Suzuki,† Shiro Ito,† Yasushi Tomita,† Junji Tanaka,‡ and Hiroshi Shimizu*

*Department of Dermatology, Hokkaido University Graduate School of Medicine, Sapporo, Japan; †Department of Dermatology, Nagoya University Graduate School of Medicine, Nagoya, Japan; ‡Department of Hematology and Oncology, Hokkaido University Graduate School of Medicine, Sapporo, Japan

Hermansky–Pudlak syndrome (HPS) is an autosomal recessive disorder characterized by oculocutaneous albinism, a bleeding disorder, and ceroid lipofuscinosis in the lungs and gut. HPS is genetically heterogeneous and the most common variant, HPS type 1, is caused by mutations in *HPS1* gene. The protein encoded by *HPS1* is considered to facilitate the trafficking of melanocyte-specific gene products into the premelanosome. We report the ultrastructural findings in a melanocytic nevus seen in a 17-y-old Japanese female patient with HPS1 who is a compound heterozygote of *HPS1* mutations, including a novel mutation. Electron microscopy of a pinkish papule corresponding to the melanocytic nevus revealed markedly aberrant, immature melanosomes, large membranous structures, and giant melanosomes in the vicinity of trans-Golgi network, the characteristic abnormalities because of protein trafficking defects in *HPS1*. These ultrastructural features were far more clearly demonstrated in the nevus cells than in the epidermal melanocytes. Thus, ultrastructural analysis of nevus cells may be an additional diagnostic tool for HPS1 and could give us important clues to further understanding of the pathomechanisms of HPS.

Key words: Chediak–Higashi syndrome/melanocyte/vesicle formation
J Invest Dermatol 125:154–158, 2005

Hermansky–Pudlak syndrome (HPS; MIM 203300) is a rare, autosomal recessive disorder characterized by oculocutaneous albinism, bleeding diathesis, and lysosomal accumulation of ceroid lipofuscin. HPS was first described by Hermansky and Pudlak (1959). Mutations in seven genes, *HPS*1–7 have been identified to cause HPS in humans (Oh *et al*, 1996; Dell'Angelica *et al*, 1999; Anikster *et al*, 2001; Suzuki *et al*, 2002; Li *et al*, 2003; Zhang *et al*, 2003) and *HPS1* is the most common causative gene.

Proteins encoded by *HPS* genes are thought to be involved in trafficking of lysosome proteins and lysosome-related organelles, and abnormalities of lysosomes and other specific organelles, such as platelet dense granules, lung lamellar bodies, and melanosomes, have been observed during light and electron microscopic examination. Melanocytes in HPS contain predominantly premature melanosomes and abnormal, large membranous structures including tubulovesicular structures because of these trafficking defects (Witkop *et al*, 1973; Frenk and Lattion, 1982; Boissy *et al*, 1998; Husain *et al*, 1998).

In this study, we demonstrated ultrastructural features of the nevus cells from an HPS patient harboring one novel and one recurrent HPS1 mutations. The present findings seen in the nevus cells could provide us significant information for the diagnosis of HPS.

Abbreviations: CHS, Chediak–Higashi syndrome; HPS, Hermansky–Pudlak syndrome

Results

Clinical presentation The patient was a 17-y-old Japanese female. She was the second child of non-consanguineous, healthy parents. There was no family history of genodermatosis including albinism. She had one unaffected elder sister. She had presented with oculocutaneous albinism since birth and had a history of easy bruising. No infectious diathesis was noted. On physical examination, we noted that her skin was extraordinarily pale for a Japanese patient, and her hair was pale blonde (Fig 1*a*). Her eyes were pale red-brown. Ophthalmologic examination revealed mild horizontal nystagmus and slightly reduced visual acuity. A round, pinkish papule, measuring 5 mm in diameter, was seen on her neck (Fig 1*b*). The papule was resected and processed for morphological observation. Laboratory examination showed decreased platelet aggregation to collagen. Chest computed tomography demonstrated no evidence of interstitial pneumonitis. Gastrointestinal and colon endoscopies revealed no abnormality and granulomatous colitis was excluded.

HPS gene mutation analysis The mutation analysis for her *HPS1* gene revealed that the patient was a compound heterozygote for a novel mutation IVS6+1G>A (Fig 2*a*) (sequence according to GenBank accession No. AF450133) and a recurrent *HPS1* mutation IVS5+5G>A (Fig 2*b*), which has been reported in Japanese HPS patients (Oh *et al*, 1998; Horikawa *et al*, 2000). We previously reported

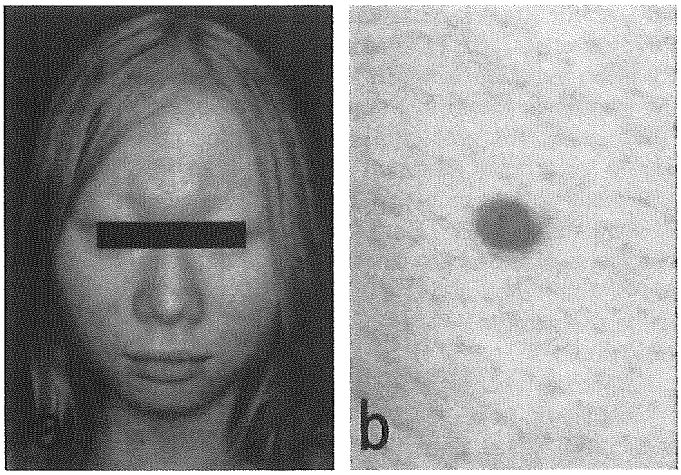

Figure 1
Clinical features of the Hermansky–Pudlak Syndrome 1 patient. (*a*) The face of the patient. The skin is pale and the hair is bright gold in color as a Japanese girl. Her eyes are pale red-brown (not shown). (*b*) A pinkish papule, melanocytic nevus, 5 mm in diameter, was present on her neck.

that IVS5 + 5G > A is a pathologic mutation with an experimental evidence, which results in the exon 5 skipping (Suzuki *et al*, 2004). Then we investigated an aberrant splice pattern caused by the IVS6 + 1G > A mutation with the RT-PCR method using the patient RNA. The allele with the IVS6 + 1G > A mutation was amplified with primers spanning around exons 5–7. This primer set would not amplify the transcript derived from another allele with IVS5 + 5G > A which defected exon 5 because of the exon 5 skipping. The result showed that, in the transcript, next GT site within intron 6 (IVS6 + 44) was used for a splice donor site, resulting in a frameshift in the mutant mRNA (Fig 2*c*).

Histological and ultrastructural findings of a pigmented nevus in HPS Light microscopy of the skin sample from the papule of the patient showed that cuboidal or oval cells with round nuclei were clustered in the dermis (Fig 3*a*). A small number of nevus cells contained melanin pigment (Fig 3*b*). Electron microscopy revealed that melanocytes in the epidermis contained mainly premature melanosomes in the cytoplasm, although a few electron dense, mature melanosomes were seen (Fig 4*a*). Most of the melanosomes were in stage I or II, and stage IV melanosomes were rarely seen.

The nevus cells in the dermis contained abundant vesicles of a similar size to that of normal melanosomes (Fig 4*b*), ceroid-like structures and electron-dense pigment within these vesicles (Fig 4*c*), whereas only a small number of those vesicles were also observed in the epidermal melanocytes (Fig 4*a*). In addition, remarkable, large electron-dense structures, 0.7 μm in diameter were seen at the periphery of the trans-Golgi network (Fig 4*d*). These abnormal structures, included large membranous structures, large

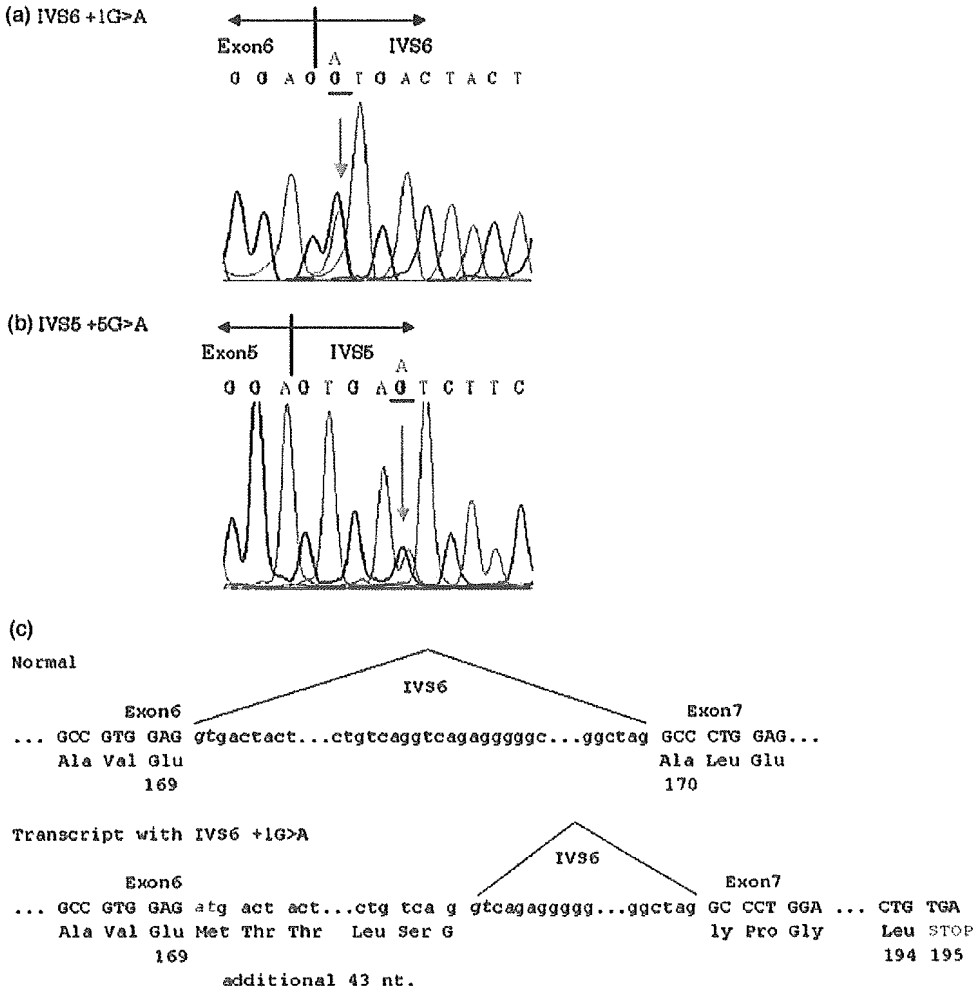

Figure 2
HPS gene mutations and altered splicing in the patient. Direct DNA sequence analysis of the splice donor sites in IVS6 (*a*) and IVS5 (*b*) in the *HPS1* gene. In IVS6, + 1G > A was detected and in IVS5, + 5G > A mutation was identified. (*c*) A mutation of G to A at the first base of IVS6 abolished the 5′ splice site. RT-PCR and DNA sequence analysis showed that the corresponding mRNA was aberrantly spliced, using a cryptic 5′ splice site within IVS6, which resulted in a frameshift.

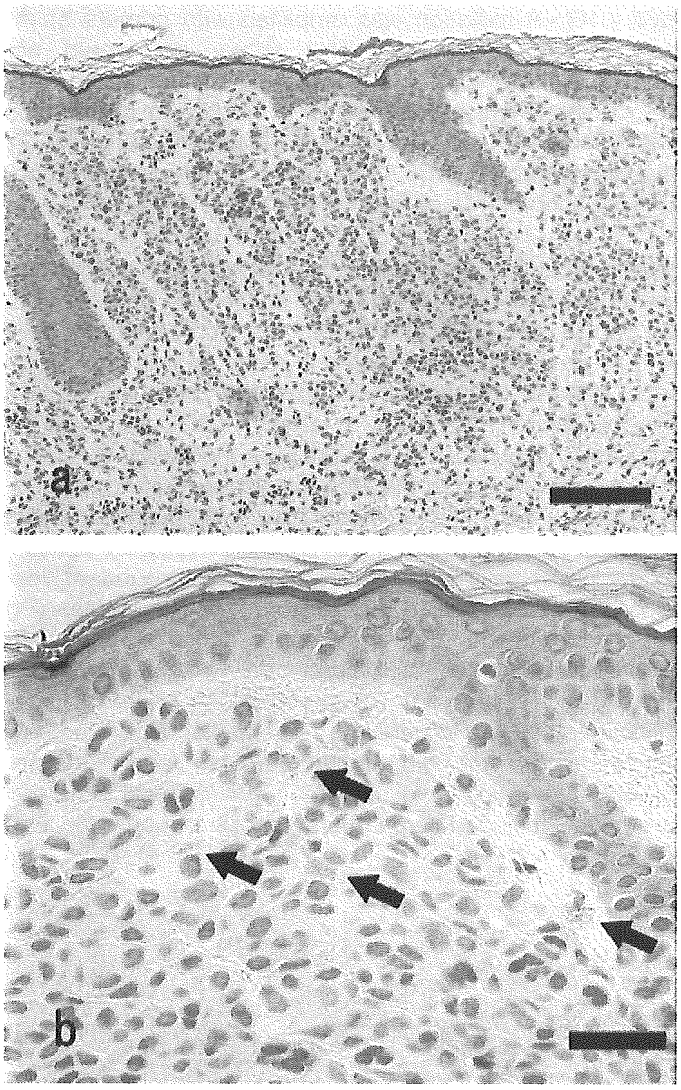

Figure 3
Microscopic features of the pinkish melanocytic nevus on her neck. (*a*) Abundant nevus cells are aggregated in the dermis (hematoxylin and eosin, *scale bar*: 80 μm). (*b*) A few nevus cells contain melanin pigment (*arrows*) (hematoxylin and eosin, *scale bar*: 30 μm).

electron-dense structures, and immature vesicles were remarkably abundant in the nevus cells compared with other cells including epidermal melanocytes.

Electron microscopy showed that, in a control melanocytic nevus of a healthy female, mature melanosomes were scattered and partly aggregated presumably as autophagic vacuoles in the cytoplasm (Fig 4*e*). Neither giant melanosomes nor aberrant vesicles were observed.

Discussion

HPS comprises a group of heterozygous disorders that result from abnormal vesicle formation and protein trafficking. At least, seven human HPS subtypes have been identified (HPS1–7).

HPS1 gene was mapped 10q23 (Fukai *et al*, 1995; Wildenberg *et al*, 1995). It has an open reading frame of 2103 bp, and is divided into 20 exons (Oh *et al*, 1996). To date, about 20 gene mutations in *HPS1* have been reported (Hermos *et al*, 2002; Huizing and Gahl, 2002), and the most common mutation in *HPS1* is a 16 bp duplication in exon 15, frequently found in Puerto Rican pedigrees (Oh *et al*, 1996, 1998). The present patient was a compound heterozygote for a novel mutation of *HPS1*, IVS6+1G>A and a previously known mutation, IVS5+5G>A (Oh *et al*, 1998; Horikawa *et al*, 2000). Both mutations are splice donor site mutations. Besides the present case, only one splice acceptor site mutation IVS17−2A>C has been reported as a splice mutation in *HSP1* (Oetting and King, 1999; Hermos *et al*, 2002).

Abnormal melanosomes have been reported in HPS patients (Witkop *et al*, 1973; Frenk and Lattion, 1982; Boissy *et al*, 1998; Husain *et al*, 1998) and in murine models of HPS (Nguyen and Wei, 2004). HPS1 protein has been thought to function in trafficking molecules to lysosome-related organelles and to be closely related to the formation of lysosome-related organelles. Especially in melanocytes, the HPS1 protein was thought to be involved in sorting melanosome-specific molecules and in formation of early vesicles (premelanosomes) from the trans-Golgi network (Huizing and Gahl, 2002). Previous reports also revealed that melanocytes in HPS patients had exclusively premature melanosomes (Witkop *et al*, 1973; Frenk and Lattion, 1982; Boissy *et al*, 1998; Husain *et al*, 1998). Because of the fact that nevus cells frequently show high melanin producing activity, we hypothesized that melanocytic nevus might show exaggerated abnormalities compared with melanocytes in the epidermis.

Our ultrastructural observation of nevus cells in the HPS patient revealed abnormal vesicles, large membranous structures, and large electron-dense structures, whereas those structures were scarcely seen in epidermal melanocytes of the patient. Many of those abnormal structures retained small amount of pigmentation, elliptical shape, or striations characteristic to melanosomes, and they were thought to be aberrant melanosomes, although we could not excluded the possibility that some of the vesicles were of lysosomal origin. These include abnormal immature melanosomes, large membranous structures, and remarkable large electron-dense structures (giant melanosomes), which were observed abundantly in the periphery to the trans-Golgi network and were thought to be representing trafficking defects, characteristic to HPS. We have utilized genetic analysis and blood clotting assessment for the diagnosis of HPS, and it is true those tests are highly useful. We think ultrastructural analysis of nevus cells can be used as an additional diagnostic procedure.

Giant melanosomes have also been demonstrated in melanocytes from non-Puerto Rican HPS patients (Frenk and Lattion, 1982; Lattion *et al*, 1983; Schallreuter *et al*, 1993; Horikawa *et al*, 2000). Among the patients showing giant melanosomes, mutations were detected only in two patients and both patients had identical mutations, IVS5+5G>A. Those abnormal melanosomes have never been observed in Puerto Rican HPS patients. Horikawa *et al* (2000) speculated that this distinction might be because of the HPS1 gene mutation sites and nature of the defects. Mutation site and/or the nature of IVS5+5G>A lesion might affect vesicle–vesicle fusion, which would result in the

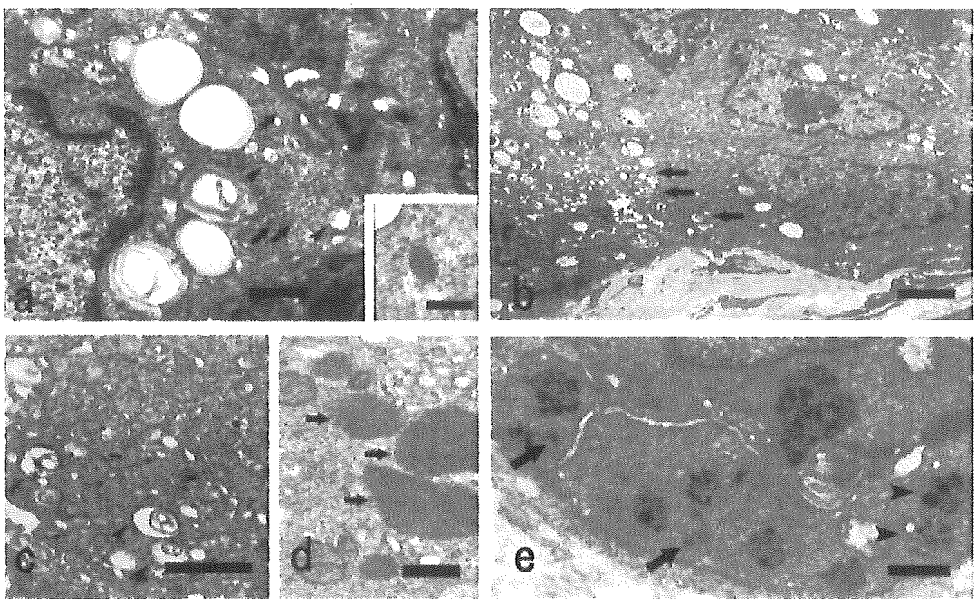

Figure 4
Electron microscopic features of the pinkish melanocytic nevus in Hermansky–Pudlak syndrome 1 patient. (*a*) In the epidermal melanocytes, the majority of melanosomes were in stage I or II (*arrows*) (*scale bar*: 5 μm). A few vesicles (*arrowheads*) were observed. A small number of mature melanosomes were seen (*inset*, *scale bar*: 0.4 μm). (*b*) In the dermal nevus cells, a large number of vacuoles and vesicles (*arrows*) were seen (*scale bar*: 2 μm). (*c*) Vesicles of a similar size to melanosomes (*arrowheads*) were seen and ceroid-like structures and electron-dense pigments were observed in these vesicles (*scale bar*: 1 μm). (*d*) Remarkable large, electron-dense structures (*arrows*), putative giant melanosomes were seen close to the trans-Golgi network (*scale bar*: 0.3 μm). (*e*) In the control nevus cells, abundant mature melanosomes (*arrows*) were observed, and some of those melanosomes were aggregated (*arrowheads*) (*scale bar*: 4 μm). There were no giant melanosomes and abnormal vesicles.

formation of large membranous structures and giant melanosomes as observed in the nevus cells in our HPS patient.

Interestingly, giant melanosomes are also seen in patients with Chediak–Higashi syndrome (CHS), a lysosomal disorder that also presents as oculocutaneous albinism, similar to HPS (Zelickson *et al*, 1967). CHS protein is considered to be a negative regulator of vesicle–vesicle fusion and impaired CHS protein function that promotes formation of large vesicles, such as giant melanosomes (Huizing *et al*, 2001; Marks and Seabra, 2001).

To our knowledge, this is the first report describing ultrastructural features of a nevus cell in an HPS patient. This study revealed that characteristic abnormalities because of protein trafficking defects, aberrant immature melanosomes, large membranous structures, and remarkable large electron-dense structures in the vicinity of the trans-Golgi network, were more clearly demonstrated in the cells in the melanocytic nevus than in other cell types including the epidermal melanocytes. These characteristic ultrastructural findings in nevus cells could provide important clues to further understanding of the pathomechanism of HPS.

Materials and Methods

Mutation detection Using a genomic DNA purification kit (QIAGEN, Valencia, California), genomic DNA was isolated from peripheral blood of the patient. Her *HPS1* gene was amplified from her genomic DNA by PCR using the primers and PCR conditions described previously (Bailin *et al*, 1997). The amplified fragments were then screened for mutations by simultaneous analyses of single-stranded conformation polymorphisms and heteroduplexes method (Spritz *et al*, 1992). PCR products showing aberrant patterns were reamplified and sequenced directly. For RT-PCR analysis RNA was extracted from mononuclear cells in the peripheral blood. The primers for RT-PCR were EX5cf; 5′-TGTGGACGGTCATCTTATCC-3′ in exon 5 and EX7cr; 5′-GGTGTTGACAGCCTGGATGA-3′ in exon 7.

Ultrastructural observations A papule on the patient's neck was resected for morphological observation. In addition, a skin sample of a control melanocytic nevus was obtained from a 29-y-old unrelated female. The pigmented lesion had been present on her back for 10 y. Skin biopsy samples were fixed in 2% glutaraldehyde solution, post-fixed in 1% OsO_4, dehydrated, and embedded in Epon 812 (Perry *et al*, 1987). The samples were sectioned at 1 μm thickness for light microscopy and thin sectioned for electron microscopy (70 nm thick). The histological sections were stained by the method of Richardson *et al* (1960). The thin sections were stained with uranyl acetate and lead citrate (Reynolds, 1963) and examined in a transmission electron microscope.

The medical ethical committee of Hokkaido University approved all described studies. The study was conducted according to Declaration of Helsinki Principles. Participants gave their written informed consent.

DOI: 10.1111/j.0022-202X.2005.23743.x

Manuscript received August 5, 2004; revised January 19, 2005; accepted for publication January 24, 2005

Address correspondence to: Ken Natsuga, MD, Department of Dermatology, Hokkaido University Graduate School of Medicine, North 15 West 7, Kita-ku, Sapporo 060-8638, Japan. Email: natsuga@med.hokudai.ac.jp

References

Anikster Y, Huizing M, White J, *et al*: Mutation of a new gene causes a unique form of Hermansky–Pudlak syndrome in a genetic isolate of central Puerto Rico. Nat Genet 28:376–380, 2001

Bailin T, Oh J, Feng GH, Fukai K, Spritz RA: Organization and nucleotide sequence of the human Hermansky–Pudlak syndrome (HPS) gene. J Invest Dermatol 108:923–927, 1997

Boissy RE, Zhao Y, Gahl WA: Altered protein localization in melanocytes from Hermansky–Pudlak syndrome: Support for the role of the HPS gene product in intracellular trafficking. Lab Invest 78:1037–1048, 1998

Dell'Angelica EC, Shotelersuk V, Aguilar RC, *et al*: Altered trafficking of lysosomal proteins in Hermansky–Pudlak syndrome due to mutations in the 3A subunit of the AP-3 adaptor. Mol Cell 3:11–21, 1999

Frenk E, Lattion F: The melanin pigmentary disorder in a family with Hermansky–Pudlak syndrome. J Invest Dermatol 78:141–143, 1982

Fukai K, Oh J, Frenk E, Almodovar C, Spritz RA: Linkage disequilibrium mapping of the gene for Hermansky–Pudlak syndrome to chromosome 10q23.1–q23.3. Hum Mol Genet 4:1665–1669, 1995

Hermansky F, Pudlak P: Albinism associated with hemorrhagic diathesis and unusual pigmented reticular cells in the bone marrow: Report of two cases with histochemical studies. Blood 14:162–169, 1959

Hermos CR, Huizing M, Kaiser-Kupfer MI, Gahl WA: Hermansky–Pudlak syndrome type 1: Gene organization, novel mutations, and clinical-molecular review of non-Puerto Rican cases. Hum Mutat 20:482, 2002

Horikawa T, Araki K, Fukai K, Ueda M, Ueda T, Ito S, Ichihashi M: Heterozygous *HPS1* mutations in a case of Hermansky–Pudlak syndrome with giant melanosomes. Br J Dermatol 143:635–640, 2000

Huizing M, Anikster Y, Gahl WA: Hermansky–Pudlak syndrome and Chediak–Higashi syndrome: Disorders of vesicle formation and trafficking. Thromb Haemost 86:233–245, 2001

Huizing M, Gahl WA: Disorders of vesicles of lysosomal lineage: The Hermansky–Pudlak syndromes. Curr Mol Med 2:451–467, 2002

Husain S, Marsh E, Saenz-Santamaria MC, McNutt NS: Hermansky–Pudlak syndrome: Report of a case with histological, immunohistochemical and ultrastructural findings. J Cutan Pathol 25:380–385, 1998

Lattion F, Schneider P, Da Prada M, Lorez HP, Richards JG, Picotti GB, Frenck E: Hermansky–Pudlak syndrome in a Valais village. Helv Paediatr Acta 38:495–512, 1983

Li W, Zhang Q, Oiso N, *et al*: Hermansky–Pudlak syndrome type 7 (HPS-7) results from mutant dysbindin, a member of the biogenesis of lysosome-related organelles complex 1 (BLOC-1). Nat Genet 35:84–89, 2003

Marks MS, Seabra MC: The melanosome: Membrane dynamics in black and white. Nat Mol Rev Cell Biol 2:738–748, 2001

Nguyen T, Wei ML: Characterization of melanosomes in murine Hermansky–Pudlak syndrome: Mechanisms of hypopigmentation. J Invest Dermatol 122:452–460, 2004

Oetting WS, King RA: Molecular basis of albinism: Mutations and polymorphisms of pigmentation genes associated with albinism. Hum Mutat 13:99–115, 1999

Oh J, Bailin T, Fukai K, *et al*: Positional cloning of a gene for Hermansky–Pudlak syndrome, a disorder of cytoplasmic organelles. Nat Genet 14:300–306, 1996

Oh J, Ho L, Ala-Mello S, *et al*: Mutation analysis of patients with Hermansky–Pudlak Syndrome: A frameshift hot spot in the HPS gene and apparent locus heterogeneity. Am J Hum Genet 62:593–598, 1998

Perry TB, Holbrook KA, Hoff MS, Hamilton EF, Senikas V, Fisher C: Prenatal diagnosis of congenital nonbullous ichthyosiform erythroderma (lamellar ichthyosis). Prenat Diag 7:145–155, 1987

Reynolds ES: The use of lead citrate at high pH as an electron-opaque stain in electron microscopy. J Cell Biol 17:208–212, 1963

Richardson KC, Jarett L, Finke EH: Embedding in epoxy resins for ultrathin sectioning in electron microscopy. Stain Technol 35:313–323, 1960

Schallreuter KU, Frenk E, Wolfe LS, Witkop CJ, Wood JM: Hermansky–Pudlak syndrome in a Swiss population. Dermatol 187:248–256, 1993

Spritz RA, Holmes SA, Ramesar R, Greenberg J, Curtis D, Beighton P: Mutations of the KIT (mast/stem cell growth factor receptor) proto-oncogene account for a continuous range of phenotypes in human piebaldism. Am J Hum Genet 51:1058–1065, 1992

Suzuki T, Ito S, Inagaki K, Suzuki N, Tomita Y, Yoshino M, Hashimoto T: Investigation on the IVS5 + 5G → A splice site mutation of *HPS1* gene found in Japanese patients with Hermansky–Pudlak syndrome. J Dermatol Sci 36:106–8, 2004

Suzuki T, Li W, Zhang Q, *et al*: Hermansky–Pudlak syndrome is caused by mutations in HPS4, the human homolog of the mouse light-ear gene. Nat Genet 30:321–324, 2002

Wildenberg SC, Oetting WS, Almodovar C, Krumwiede M, White JG, King RA: A gene causing Hermansky–Pudlak syndrome in a Puerto Rican population maps to chromosome 10q2. Am J Hum Genet 57:755–765, 1995

Witkop CJ Jr, Hill CW, Desnick S, *et al*: Ophthalmologic, biochemical, platelet, and ultrastructural defects in the various types of oculocutaneous albinism. J Invest Dermatol 60:443–456, 1973

Zelickson AS, Windhorst DB, White JG, Good RA: The Chediak–Higashi syndrome: Formation of giant melanosomes and the basis of hypopigmentation. J Invest Dermatol 49:575–580, 1967

Zhang Q, Zhao B, Li W, *et al*: Ru2 and Ru encode mouse orthologs of the genes mutated in human Hermansky–Pudlak syndrome types 5 and 6. Nat Genet 33:145–153, 2003

Available online at www.sciencedirect.com
SCIENCE DIRECT®
Bioresource Technology 96 (2005) 1955–1958
BIORESOURCE TECHNOLOGY

Short Communication

Production of mesoscopically patterned cellulose film

Junji Nemoto [a], Yasumitsu Uraki [a,*], Takao Kishimoto [a], Yuzo Sano [a], Ryo Funada [a], Noriaki Obata [b], Hiroshi Yabu [b,e], Masaru Tanaka [c,d], Masatsugu Shimomura [b,e]

[a] *Graduate School of Agriculture, Hokkaido University, Kita-9, Nishi-9, Kita-ku, Sapporo 060-8589, Japan*
[b] *Nanotechnology Research Center, Research Institute for Electronic Science (RIES), Hokkaido University, Kita-12, Nishi-6, Kita-ku, Sapporo 060-0812, Japan*
[c] *Creative Research Initiative "Sousei" (CRIS), Hokkaido University, N-21, W-10, Kta-ku, Sapporo 001-0021, Japan*
[d] *Precursory Research for Embryonic Science and Technology (PRESTO), Japan Science and Technology Corporation (JST), N-21, W-10, Kta-ku, Sapporo 001-0021, Japan*
[e] *Core Research for Evolutional Science and Technology (CREST), Japan Science and Technology Corporation (JST), N-21, W-10, Kta-ku, Sapporo 001-0021, Japan*

Received 12 January 2004; received in revised form 19 January 2005; accepted 19 January 2005
Available online 19 March 2005

Abstract

Honeycomb and stripe patterned films were prepared from cellulose triacetate (CTA)/chloroform solution, as a result of the self-organization of the polymer during evaporation of the solvent. The honeycomb patterned CTA films were prepared by two methods, a direct pattern formation method and a transcription method. The latter method gave a well-organized microporous honeycomb pattern. Both types of patterned CTA films were saponified to yield the corresponding patterned cellulose films.

Keywords: Honeycomb pattern; Stripe pattern; Self-organization; Cellulose; Cellulose acetate

1. Introduction

Patterned films with regulated structure in nano- and micro-orders formed by self-organization processes have drawn much attention with potential applications in the fields of electronics (Imada et al., 1999), photonics (Wijnhoven and Vos, 1998; Kurono et al., 2002), biomaterials (Nishida et al., 2002), and so on. This fabrication technique is expected to become an alternative to lithography (Chen and Pépin, 2001). The patterned films, such as honeycomb (Widawski et al., 1994; Stenzel, 2002; Nishikawa et al., 2003; Yabu et al., 2003) and stripe and ladder (Maruyama et al., 1998; Karthaus et al., 1999, 2001; Yabu et al., 2002; Shimomura et al., 2003) were spontaneously formed by casting polymer solutions on solid substrates, followed by solvent evaporation. Such films have been produced from synthetic polymers. Taking environmental problem and petroleum supplies into consideration, it could be useful to prepare patterned films from natural polymers.

Cellulose is the most abundant, naturally occurring polymer. Porous cellulose films have already been produced for separation and dialysis in industry and medicine on the basis of hydrophilicity and biocompatibility (Miyamoto et al., 1989; Risbud and Bhonde, 2001). If the patterned films were manufactured from cellulose, they could be used for not only conventional applications but also novel uses of biomass-derived feed stocks.

According to previous reports (Widawski et al., 1994), the honeycomb pattern was fabricated from a solution of polymer in water-immiscible solvents under high humidity on the basis of self-organization of

* Corresponding author. Tel.: +81 11 706 2817; fax: +81 11 716 0879.
E-mail address: uraki@for.agr.hokudai.ac.jp (Y. Uraki).

0960-8524/$ - see front matter © 2005 Elsevier Ltd. All rights reserved.
doi:10.1016/j.biortech.2005.01.034